Tailored out-of-oven energy efficient manufacturing of high performance composites with two-stage self-regulating heating via double positive temperature coefficient effect

*Xudan Yao [a,b,**], Yushen Wang [a], Thomas D. S. Thorn [a], Shanshan Huo [a], Dimitrios G. Papageorgiou [a], Yi Liu [c], Emiliano Bilotti [a], Han Zhang [a,*]*

[a] School of Engineering and Materials Science, Queen Mary University of London, London E1 4NS, UK

[b] School of Aeronautics, Northwestern Polytechnical University, Xi'an 710072, China

[c] Department of Materials, Loughborough University, Loughborough LE11 3TU, UK

* Corresponding author: han.zhang@qmul.ac.uk x.yao@nwpu.edu.cn

Keywords: sustainable manufacturing; conductive polymer composite; nanocomposites; graphene nanoplatelets; out-of-oven curing

Abstract

The needs for sustainable development and energy efficient manufacturing are crucial in the development of future composite materials. Out-of-oven (OoO) curing of fibre reinforced composites based on smart conductive polymers reduces energy consumption and self-regulates the heating temperature with enhanced safety in manufacturing, presenting an excellent example of such energy efficient approaches. However, achieving the desired curing processes, especially for high performance systems where two-stage curing is often required,

remains a great challenge. In this study, a ternary system consisting of graphene nanoplatelets/HDPE/PVDF was developed, with a double positive temperature coefficient (PTC) effect achieved to fulfil stable self-regulating heating at two temperatures (120°C and 150 °C). Systematic studies on both single and double PTC effects were performed, with morphological analysis to understand their pyroresistive behaviours. Compared to the oven curing process, up to 97% reduction on the energy consumption was achieved by the ternary system while comparable thermal and mechanical properties were obtained in the carbon fibre/epoxy laminates. This work presents a new route to achieve OoO curing with two-stage self-regulating heating, which can be utilised in many high performance composite applications.

1. Introduction

With the increasing concerns over the environmental impact of industrial processes, novel technologies and materials with high energy efficiency and low carbon footprints are increasingly in demand. Thanks to the high specific strength and stiffness, as well as good chemical resistance, fibre reinforced plastics (FRPs) have been widely used as an environmentally friendly lightweight solutions in diverse fields, such as aerospace, automotive, civil, energy, and sports. Unfortunately, the manufacturing of advanced composites using traditional methods, such as autoclave and oven-based curing processes, often leads to high energy consumption and size restrictions.

To overcome these limitations, out-of-oven (OoO) curing methods have gained much attention in recent years, ranging from microwave heating [1–4], induction heating [4–6], frontal

polymerisation [7–9], heated tooling [10–12], to resistive heating. In particular, resistive heating (or Joule heating), especially the use of a surface conductive layer such as carbon nanotubes or graphene, has been explored as one of the promising methods owing to its high compatibility with existing fibre/matrix system, and ease of fabrication compared to integrally heated tooling. A wide range of resistive heating layers have been studied, such as carbon nanotube (CNT) film [13-16], graphene film [17-20], conductive wires [21], etc. However, the associated risks of overheating and burning from the excellent heating performance of many resistive heating systems should not be overlooked. The risks of malfunction or failure in the temperature controller, such as a PID controller, for the feedback loop in heated tooling also should not be overlooked, as they could lead to substantial heat-related hazards or production disruptions. The development of smart conductive heating layer that can self-regulate their heating temperatures presents a novel and exciting avenue for the sustainable manufacturing of composites.

Very recently, our group has conducted studies on the pyroresistive performance of conductive polymer composites (CPC), leading to the development of reliable self-regulating heating performance which can be utilised for sustainable OoO curing with *in-situ* temperature adjustment [22-27]. By employing a single-step positive temperature coefficient (PTC) effect, which involves a sharp increase in the electrical resistance of the CPC due to the polymer matrix thermal expansion at the switching temperature (T_{sw}), the heating can be self-regulated without overheating due to the disconnection of conductive pathways. When the temperature drops below T_{sw}, the polymer shrinks back, reconnecting the conductive pathways and resuming the heating with the temperature under control [25,27]. Compared to composites cured

by traditional oven heating, OoO curing requires only a few percentages of energy consumption, which significantly contributes to the sustainable manufacturing of composite materials [22,27], especially considering the growing demand of advanced composites. The integrated CPC layer used in OoO curing also can be utilised as an embedded smart surface layer, providing additional functions ranging from structural health monitoring to de-icing, towards a multifunctional lightweight composite structure.

However, the capability of self-regulate the heating at one switching temperature also poses a challenge for high performance FRPs, whereas a two-stage curing process is often required with a post curing step at elevated temperature beyond the first stage. Unfortunately, the single PTC effect with an autonomous cut-off of conductive pathways cannot fulfil the needs of post curing at a further elevated temperature. To solve this challenge, a double (two-step) PTC effect needs to be developed to fulfil the requirement. Different routes have been explored to achieve the double PTC effect over the last years. Zhang *et al.* filled HDPE with Sb-Pb alloy, and achieved double PTC effects owing to different melting points of the polymer matrix and alloy fillers [28,29]. The introduction of a secondary filler, such as VO_2 which has the phase-transformation characteristic changing from semiconductor to metal at around 68 °C, contributed to the double PTC effect in graphite/HDPE composites as reported by Zhang *et al.*[30,31] Binary polymer matrix nanocomposites based on polymer blends with a two-stage thermal expansion hence two stages of resistance jump have also been explored [32-34]. Feng *et al.* [34] proposed the type I + M (Interface + Matrix) conductive pathway theory by combining carbon black (CB), polypropylene (PP) and ultrahigh molecular weight polyethylene (UHMWPE) via melt processing, and studied the effect of PP/UHMWPE ratio on the PTC

intensities of each stage. Wei *et al.* [33] manufactured conductive CB/PP/UHMWPE composites via a different processing method: grinding and solution mixing, followed by hot compaction, with an ultra-low percolation threshold achieved owing to the segregated structure. Zhang *et al.* [32] used carbon nanofibre (CNF), HDPE and PVDF with different matrix volume ratios, and only obtained double PTC at 1/4 ratio with a relatively low PTC intensity of the second step, explained by the "island-bridge" theory. The second PTC effect was attributed to the thermal expansion of PVDF which broke the CNF "bridges" between CNF/HDPE "islands". As the separation of conducting pathways from this stage is much less than the first stage when HDPE expands and separated the network within the "islands", the PTC intensity of second stage was much lower than the first stage. In order to achieve a reliable two-step control on self-regulating heating, a sufficient PTC intensity is required for both stages.

To achieve a clear PTC effect with sufficiently high intensity, semicrystalline polymers are often favoured, owing to their relatively large thermal expansions when approaching their melting temperatures of the crystalline phase [23,25]. Hence, two semicrystalline polymers, HDPE and PVDF, with distinct melting points (~130°C and ~175 °C) are utilised in this work to fulfil the two-step curing cycle requirements. Apart from the PTC effect, Joule heating is another function that is vital for OoO curing, which ideally needs both high PTC intensity for smart switching and appropriate resistance for Joule heating. Regarding the conductive filler selection, Liu *et al.* [23] compared 0D (silver coated glass spheres, AgS), 1D (CNT) and 2D (graphene nanoplatelet, GNP) fillers. It was found that the 0D filler tends to have the highest PTC intensity with the lowest resistivity under the highest loading due to its least number of contact points and lowest specific surface area, the 1D CNT one shows the lowest PTC

intensity owing to its 'robust' conductive networks with many entanglements that are the least likely to be broken, while the 2D GNP behaves intermediately in both PTC intensity and loading for percolation threshold.

In this study, CPC with double PTC effect is fabricated and utilised as a surface layer to cure the high performance carbon fibre/epoxy laminates, with a two-stage curing cycle. A systematic characterisation on the composite laminates cured by OoO and traditional oven method has been performed, comparing their thermomechanical, morphological and mechanical performance, while the energy consumption between two methods were also measured and compared. The results indicate that OoO cured carbon fibre (CF)/epoxy laminates possess equivalent properties to the traditional oven cured specimens, with a significantly reduced energy consumption towards the sustainable development of this field.

2. Experimental

2.1 Materials

Graphene nanoplatelets (GNPs) (XG sciences, Grade M25, USA) were used as the conductive fillers in this work, which have an average particle diameter of 25 μm, thickness of 6–8 nm (~ 20 layers of graphene) and density (ρ_g) of 2.2 g cm^{-3} according to the manufacturing datasheet. PVDF with particle size < 300 μm, density of 1.78 g cm^{-3} (Solef 1015, Belgium) and HDPE with density of 0.952 g cm^{-3} (RIGIDEX, HD5218EA, UK) were used as the polymer matrix, with the melting temperatures (T_m) at around 175 °C and 130 °C respectively, with the aim of matching the PTC switching temperatures (which are often slightly below the

T_m) to the curing cycle of the epoxy resin system (Araldite LY 1564, Aradur 2954, USA). Stitched carbon fibre fabric was obtained from Hexcel (HiMax™ FCIM151, 303 gsm, -45/+45, USA). A 300gsm non-woven heavyweight polyester felt fabric (BR180) was bought from Easy Composites Ltd (UK) and used as the thermal insulation layers during OoO curing process. All polymer matrices were dried in the oven at 80 °C overnight before processing. Strips of 3 mm wide copper tapes combined with 0.056 mm thick copper wires and meshes were used as the electrical buses to connect the samples to a power supply.

2.2 PTC nanocomposites preparation

A DSM X'plore 15 micro-compounder (the Netherlands) was used for mixing 24 wt.% GNP into polymer matrices. The compounding was carried out at 240 °C and 200 °C for PVDF and HDPE, respectively, at a speed of 50 rpm under argon for 5 min. Then the extruded filaments were cut into pellets by a Dr. Collin Strand Pelletizer Type CSG 171 (Germany). The pellets were then hot pressed into films and sheets using a Dr. Collin P300E (Germany) at 200 °C under 240 bar. For GNP/HDPE/PVDF trinary system, GNP/HDPE and GNP/PVDF pellets with a HDPE/PVDF volume ratio of 1/3 were mixed for 3 min at 240 °C by the micro-compounder. For PTC test specimens, copper meshes were embedded in the nanocomposite during the compression moulding as shown in Fig. 1a. To fabricate the Joule heating films based on developed CPC, parallel copper wires with an interval of 15 mm were embedded into the film via compression moulding (Fig. 1b), with a final film thickness of around 200 μm.

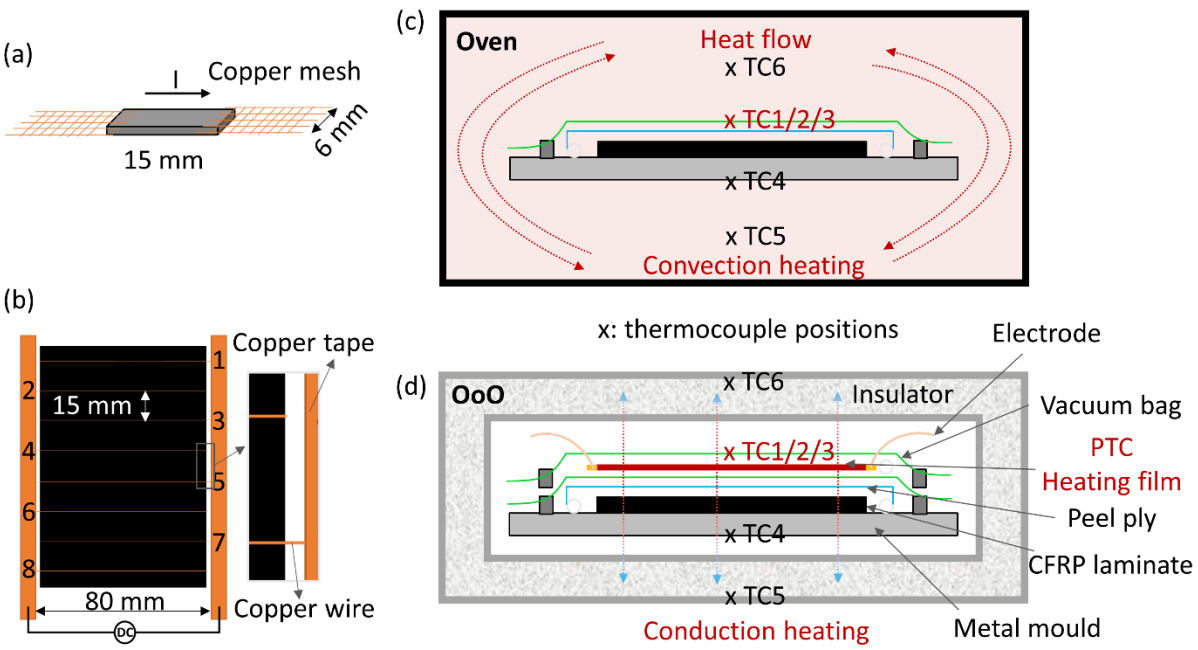

Fig. 1. Schematic illustrations of nanocomposite fabrication: (a) PTC test specimens with embedded copper mesh as electrodes; (b) Joule heating films with parallel copper wires embedded via compression moulding; (c) oven and (d) out-of-oven (OoO) with thermal couples monitoring the temperatures at various locations during the curing process. For OoO curing, the CPC film was sandwiched between two vacuum bagging layers, with a DC power supply connected for Joule heating. Thermal insulation was applied with temperatures monitored at different locations.

2.3 CF/epoxy laminate manufacturing

CF/epoxy laminates (100 mm × 100 mm) consist of 8-ply carbon fibre with a layup of $[0/90]_{2s}$ were manufactured by a vacuum assisted resin infusion (VARI). After infusion, the whole assembly was placed into an oven for curing, as shown in Fig. 1c. In comparison, considering the recyclability, reusability and cost effectiveness of OoO curing method, the heating film was

place on top of the whole VARI assembly, with another vacuum bag sealed and vacuumed to ensure the contact between smart heating film and the CF/epoxy panel (Fig. 1d). The curing cycle was based on the suggestion from the supplier, at 120 °C for 0.5 h followed by 150 °C for 2 h. Three CF/epoxy laminates were made from each curing methods.

In order to reduce the heat loss, 8 layers of polyester felt fabric were applied as the thermal insulation layers to wrap the whole assembly after infusion. Three thermocouples (TC1/2/3) were place at three different positions on the surface of the assembly to monitor the heating behaviour. One thermocouple (TC4) was adhered to the bottom surface of the stainless-steel mould. For out-of-oven curing, two additional thermocouples (TC5 and TC6) were placed between the 7^{th} and 8^{th} layer of the fabric (Fig. 1d) to monitor the heat loss. While for oven curing, TC5/6 were used to monitor the air temperature within the oven.

2.4 Characterization

A FEI Inspect F field emission scanning electron microscopy (SEM) was used to observe the morphology of GNPs and polymers, as well as cryo-fractured cross-sections of the composites. Thermogravimetric analysis (TGA 5500, TA Instruments) was used to check the final GNP loadings in the CPCs, with the samples heated up from room temperature (RT) to 800 °C at 10 °C/min under nitrogen atmosphere. Glass transition temperature (T_g) of cured CF/epoxy laminates was evaluated by differential scanning calorimetry (DSC25, TA Instruments), with temperature ramped from 40 °C to 200 °C at a heating rate of 10 °C/min under nitrogen atmosphere. Dynamic mechanical analysis (DMA Q800, TA Instruments) was performed in accordance with ASTM D7028, with the carbon fibre/epoxy specimens dimension of 56 mm x

12 mm x 1.5 mm under three point bending mode, from room temperature to 200 °C at 5 °C/min heating rate, frequency of 1 Hz, strain of 0.1% and pre-set force of 0.1 N, under air environments.

The pyroresistive behaviour of CPC smart layers was characterised by measuring the electrical resistance (Agilent 34410A 6½ Digit Multimeter) of the PTC sheets under various temperatures (monitored by K-type thermocouples and a TC-08 Pico logger) simultaneously. To examine the Joule heating performance of the film, a GE EPS 301 power supply (voltage range: 5-300 V DC; current range: 10-400 mA) was used with different voltages applied. K type thermocouples accompanied with a TC-08 thermocouple data logger from Pico Technology were used to record the temperatures of various positions on the film surfaces.

Flexural properties of carbon fibre/epoxy laminates were tested by Instron 5967 under three-point bending mode according to ASTM D7264, with the sample dimension of 60 mm x 12 mm x 1.5 mm and support span of 48 mm (span-to-thickness ratio of 32:1). The crosshead movement was set at a rate of 1.0 mm/min, with a 1kN load cell. Flexural chord modulus of elasticity was calculated using the elastic linear deformation range (e.g. strain starts from 0.001 and ends at 0.003). For each method, nine specimens in total, from three different panels were tested to ensure the repeatability of the results.

3. Results and discussion

3.1 Morphological, pyroresistive, and self-regulating heating properties of single PTC nanocomposites

Fig. 2a and 2c show the morphology of the cryo-fractured cross-sectional views of 24 wt.% GNP/HDPE and 24 wt.% GNP/PVDF nanocomposites, respectively. Continuous distribution of GNPs with sufficiently connected pathways between fillers can be found in both matrices, which can be attributed to the relatively high filler contents alongside appropriate shear force applied during the melt-mixing process. An in-plane aligned distribution of GNPs has been observed, and its formation is believed to be due to the compression moulding process.

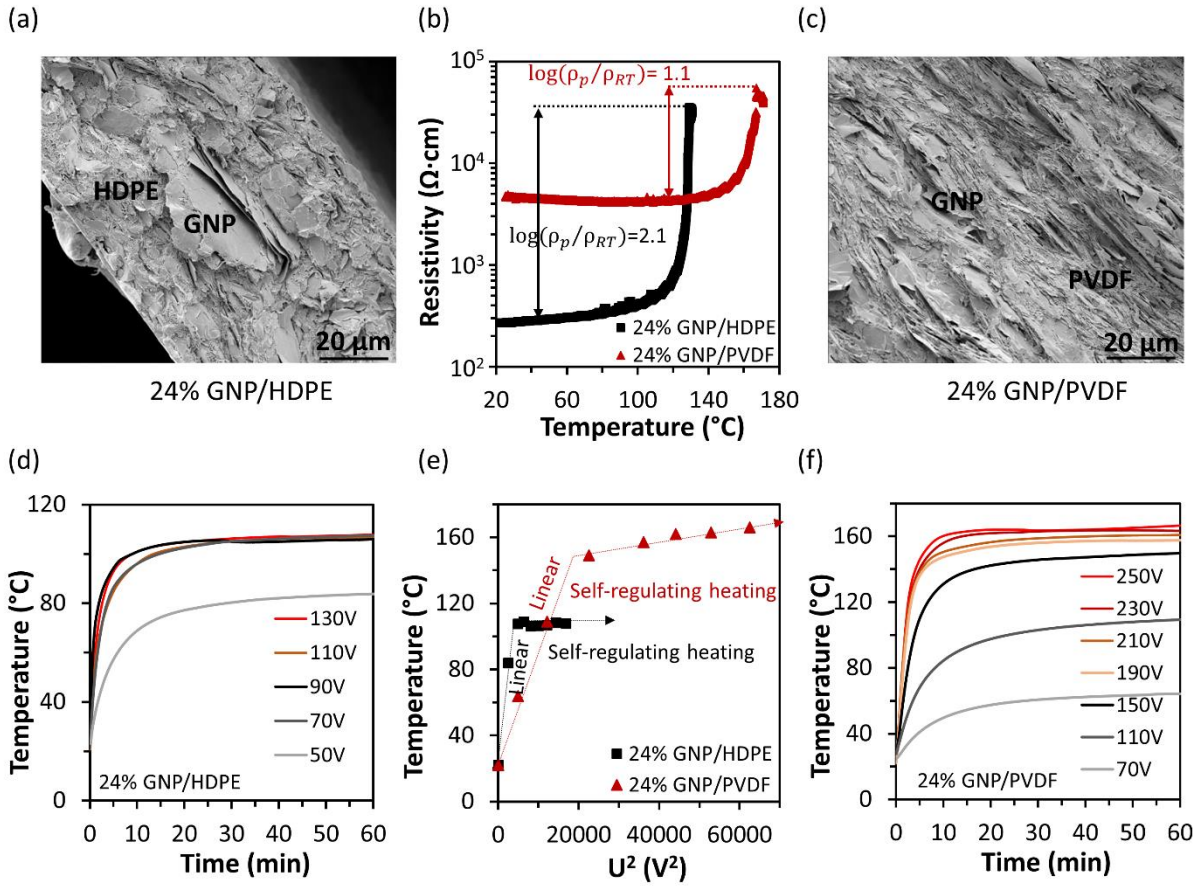

Fig. 2. SEM images of cryo-fractured cross-sections of 24 wt.% GNP in (a) HDPE and (c) PVDF, with GNPs distributed with sufficient connecting pathways inside; (b) pyroresistive behaviour of GNP/HDPE and GNP/PVDF nanocomposites, with PTC intensity of 2.1 (owing to the relatively high coefficient of thermal expansion of HDPE) and 1.1, and switching temperatures at around 120 °C and 160 °C respectively. Joule heating behaviour of (d) GNP/HDPE and (f) GNP/PVDF composites under various applied voltage. Both composites achieved self-regulating heating, with the temperatures stabilized at around 105 °C and 155 °C respectively, independent with further increased voltages, which is promising for safe manufacturing without the risk of overheating. (e) $U^2 - T$ curves of the nanocomposites, which are linear before the switching temperatures and stabilized at constants (~105 °C and ~155 °C) afterwards, confirming the self-regulating heating.

Pyroresistive behaviour of the nanocomposites was studied by monitoring their electrical resistivity changes over increased temperature. As shown in Fig. 2b, both nanocomposites show a clear single-step PTC effect, with switching temperatures at around 120 °C and 160 °C, which are attributed to the thermal expansion of the crystalline phase when approaching to the melting point of each matrix. The PTC intensity, as calculated in Equation 1 below, is 2.1 for HDPE and 1.1 for PVDF system, in agreement with their coefficient of thermal expansion (CTE) values:

$$\text{PTC intensity} = \log\left(\rho_p / \rho_{RT}\right) \quad (1)$$

Where ρ_p and ρ_{RT} are the peak and room temperature resistivity. The PTC intensity difference between 24 wt.% GNP/HDPE and 24 wt.% GNP/PVDF composites is mainly attributed to their CTE difference, where the CTE values of HDPE and PVDF are at the range of 200-250 and 110-130 respectively (10^{-6} K^{-1} at 20 °C). A higher CTE value can enable a larger volume expansion of the matrix, hence to break more conducting pathways, leading to a higher PTC intensity. It is also worth noting that, with a constant filler loading, the matrix viscosity will also influence the initial electrical conductivities due to the filler movements and re-agglomerations during the melt processing, contributing to the calculation of PTC intensity.

A relatively high PTC intensity with a clear and sharp resistance jump can contribute to the self-regulating heating performance of the nanocomposites. Both 24 wt.% GNP/HDPE and 24 wt.% GNP/PVDF composite films showed reliable self-regulating heating, as shown in Fig. 2d and 3f. For GNP/HDPE nanocomposites, with the increasing voltage applied (e.g. 50V to 70V), the peak temperature increased from 80 °C to 105 °C due to the increased power input. However, with the voltage further increased from 70 V to 90 V, 110 V or even 130 V, the peak temperature kept constant at around 105 °C (Fig. 2d), achieving a self-regulating heating. This is attributed to the PTC effect of the 24 wt.% GNP/HDPE nanocomposite. When temperature approaches the T_{sw}, the resistance of composites increased dramatically, compensating the further increased voltage inputs (U^2/R), thus led to stable output powers and prevented overheating. Similarly, for GNP/PVDF nanocomposites, a stable self-regulating heating has been observed at 155 °C (Fig. 2f), with the applied voltage increased from 190 V to 250 V.

During the Joule heating procedure, thermal insulating materials (polyester felt fabric) were used to cover the samples to prevent the major heat loss, convection [35]. In this case, energy

generated by resistive heating contributes to heat up the composite accompanied with heat loss via heat conduction and radiation, following the equations below:

$$q_{in} = \frac{U^2}{R} \tag{2}$$

$$q_{out} = c \cdot m \cdot \frac{dT(t)}{dt} + q_{cond} + q_{rad} \tag{3}$$

According to the law of conservation of energy：

$$q_{in} = q_{out} \tag{4}$$

$$\frac{U^2}{R} = c \cdot m \cdot \frac{dT(t)}{dt} + kA\frac{T_s - T_\infty}{\Delta x} + \varepsilon\sigma A(T_s^4 - T_\infty^4) \tag{5}$$

Where U is the applied voltage; t is the time; R, T, c and m are the resistance, temperature, specific heat capacity and mass of the samples; A is the heating area; T_s and T_∞ are the sample surface and environmental temperature respectively; Δx is the distance between sample surface and environment; k, ε and σ are the thermal conductivity of the insulating material, emissivity and Stefan-Boltzmann constant.

Heat radiation is proportional to the fourth power of the absolute temperature, which will become the dominate part when the temperature becomes extremely high. In this work, temperatures are relatively modest, and thus the major heat loss is through conduction. Thus, the Equation 5 could be simplified as:

$$\frac{U^2}{R} = c \cdot m \cdot \frac{dT(t)}{dt} \tag{6}$$

As a consequence, for both GNP/HDPE and GNP/PVDF nanocomposites before the switching temperatures (T_{sw}), the relationship between U^2 and T was linear, as shown in Fig. 2e. After

the T_{sw}, temperatures of both systems become stabilised without further increases (~105°C and ~155 °C), indicating the safe self-regulating heating achieved owing to the resistance jump.

3.2 Double PTC nanocomposites with two-stage self-regulating heating

In order to achieve a two-step OoO curing process for high performance FRP composites, a self-regulating heating film with a double PTC effect is of necessity. We developed a ternary nanocomposite system by melt-mixing the GNP/HDPE and GNP/PVDF at desired volume ratios, maintaining the conductive filler concentrations of 24 wt.%. Considering the difference in melting temperature between HDPE and PVDF, hence the self-regulating temperature (~105°C and ~155 °C) as observed in Fig. 2, a volume ratio of 1/3 has been chosen to achieve a continuous PVDF phase with higher switching temperature. This is to ensure the continuity of the conductive pathways as well as the matrix at elevated temperatures, especially after the first self-regulating temperature but before the second switching temperature. It is also worth noting that due to the surface tension of polymer matrix, GNPs tend to stay in HDPE rather than PVDF [23]. Therefore, a lower HDPE volume can also avoid excessive migration of GNPs from PVDF to HDPE phase. The chosen volume ratio is also expected to achieve a balanced PTC intensities between two switching temperatures, due to their different coefficient of thermal expansion and PTC intensity values.

As shown in Fig. 3a, a double PTC effect has been achieved in our GNP/HDPE/PVDF ternary nanocomposites. Upon heating, the resistance of the specimen remained stable from room temperature until around 105 °C, with a clear jump around 120 °C. With the further increased

temperature, the resistance fluctuated slightly at the same level, until a further clear jump at around 160 °C. The temperatures of these two resistance jumps are in alignment with the switching temperatures of HDPE and PVDF phases, while the calculated PTC intensity for each stage is around 0.6.

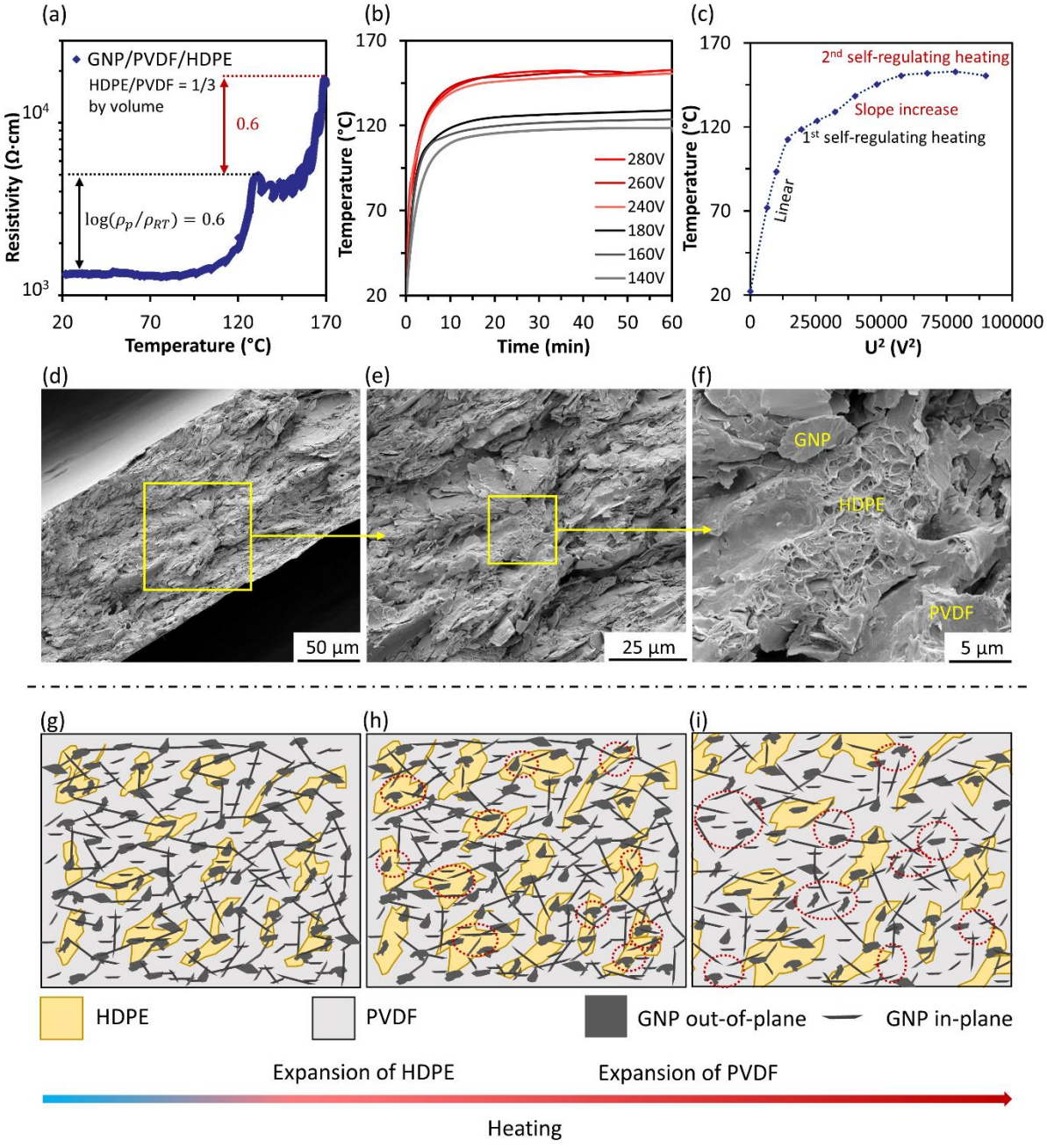

Fig. 3. 24 wt.% GNP/HDPE/PVDF ternary nanocomposites (volume ratio of HDPE and PVDF is 1:3): (a) pyroresistive properties with a clear double PTC effect; (b) Joule heating behaviour

with a two-stage self-regulating heating in accordance with two PTC switching temperatures; (c) $U^2 - T$ curve with two clear slope changes at the self-regulating temperatures (~120 °C and ~150 °C); (d-f) cross-sectional views of ternary nanocomposites, showing a continuous phase of PVDF with GNPs dispersed in both PVDF and HDPE phases, as well as their interfaces. (g-i) Schematics of the evolution of conductive networks in the ternary composites during the heating procedure, during the thermal expansion of HDPE and PVDF.

The Joule heating performance of the specimen has been examined by applying voltages at different levels, with the temperature monitored and recorded simultaneously (Fig. 3b). With the applied voltage increased from 140V to 180V, an increased heating rate has been observed due to the higher power input, while the temperature reached around 120 °C and self-regulated at that temperature without further increases. This is attributed to the thermal expansion of HDPE phase at this temperature, in consistent with first PTC switching observed. With the applied voltage further increased to a much higher level (240V), the temperature of the specimen can overcome the first regulating stage of HDPE, reaching about 150 °C and stabilised without further increase, even at a further increased voltage up to 280V. This self-regulating phenomenon at 150 °C can be attributed to the thermal expansion of PVDF phase, pushing the remained conductive pathways apart hence to restrict any further heating. These self-regulating temperatures can be tailored by changing the polymer matrix used in the nanocomposite films, aligning with the required curing temperatures of the epoxy resins. It is worth noting that the relatively high voltage applied in this work is partially due to the limited

current through the specimen (current range of 10-400 mA from the power source), which can be tuned by adjusting the film resistance between electrodes or using a higher current if needed.

As mentioned earlier in Equation 6, a linear relationship between the square of applied voltage ($\boldsymbol{U^2}$) and temperature (T) can be expected for Joule heating at current temperature range. In Fig. 3c, a linear relationship was observed at the beginning of the curve, until the temperature reaching 120 °C. A clearly reduced slope of the curve can be found at this temperature, which is due to the suddenly increased resistance of the nanocomposites at their first switching temperature (HDPE phase volume expansion). With the continued voltage square increase, the slope of the curve increased again with an increase in temperature, based on the remained conductive pathways within the PVDF phase, until the temperature reached around 150 °C where the thermal expansion of continuous PVDF phase was triggered, leading to a further resistance jump hence a self-regulated heating at this temperature. Morphological structures of current GNP/HDPE/PVDF ternary nanocomposites in Fig. 3d-i also confirmed the continuous phase of PVDF, ensuring a connected pathway for Joule heating after first self-regulating heating stage while providing a safety current cut off at the second self-regulating temperature.

In order to check the thermal behaviour and final GNP loadings of GNP/HDPE, GNP/PVDF and GNP/HDPE/PVDF, TGA was performed from RT to 800 °C at 10 °C/min, under nitrogen atmosphere, with the results summarized in Fig. S1 and Table S1. It indicates that GNPs (all at around 20 wt.%) contributed to increased decomposition temperatures owing to its high thermal stability and restriction effect, which is consistent with literatures [36,37]. In addition, the ternary nanocomposites resulted in an improved thermal stability, with a slightly higher (~20 °C) initial decomposition temperature (487.9 °C) compared with the GNP/HDPE (468.2 °C).

As the HDPE was trapped by surrounding PVDF (Fig. 3h), thermal expansion at the first switching temperature was also constrained, hence a reduced separation of conductive network until a higher temperature in GNP/HDPE/PVDF was reached (120 °C), compared with GNP/HDPE single matrix system (105 °C). In contrast, the second switching temperature dropped slightly from 155 °C (GNP/PVDF) to 150 °C (GNP/HDPE/PVDF), attributed to the synergy thermal expansion of PVDF and HDPE (Fig. 3i), which triggered an earlier cut-off of the conductive pathways.

3.3 Oven *vs* Out-of-Oven curing for high performance carbon/epoxy laminates

After successfully achieved the two-stage self-regulating heating performance based on developed GNP/HDPE/PVDF ternary nanocomposites, the heating film was fabricated and used for out-of-oven (OoO) curing of carbon/epoxy laminates with two stage curing cycles. In comparison, traditional oven was also used to cure the laminates with the same curing cycle, while the heating profiles, the mechanical and thermomechanical properties of cured laminates, as well as their energy consumption, have been compared between two curing methods.

3.3.1 Heating performance for the curing cycle

Fig. 4a compares the heating profiles between the oven and OoO curing methods, with the target cycles (dash line) of first stage at 120 °C for 30 min and second stage at 150 °C for 2 h. Both methods achieved the first curing stage from room temperature, while the OoO shows a slightly lower temperature than 120 °C. It is worth noting that this temperature for OoO method was collected from TC2, the central thermocouple attached at the outer surface of the heating

film. After the first curing stage, the temperature has been increased further to 150 °C for another two hours before cool down to room temperature. Although the heating rate of OoO method was slightly lower than oven method for the post curing stage (due to the limit of 300V could be applied from the power supply in this work), the temperature was continuous increasing until 150 °C and stabilised at that temperature. Clearly, with the laminates as well as the metal substrate underneath, a large amount of energy is required to raise the temperature, especially at the higher temperature range. It is believed with a higher voltage applied, the heating rate can be optimised for the system.

To further understand the heating performance of developed OoO method, the temperature profiles of all six thermocouples have been presented in Fig. 4b. It can be seen that all three thermocouples on the heating film surface (TC1-3 in red) show a similar profile, with one of the lines slightly below the others, especially after the first curing stage and during the entire second stage, possibly due to the locations of parallel electrodes and subsequent variation in resistance. This also explains the slightly slower ramping rate of the OoO in comparison with oven method in Fig. 4a. Decent thermal insulation has been observed for both side of the assembly (TC5 and 6), although a slightly elevated temperature can be seen from TC5 on the metal mould side, which can be attributed to the relatively compacted thermal insulation layers due to the gravity of metal mould.

It is also worth noting that the temperature of the steel mould was slightly lower (~20 °C) than the film temperature, throughout the entire curing process. This is believed due to the relatively low power density of the heating film while the relatively large thermal mass (C_{th}) of the metal plates.

$$C_{th} = \mathrm{c} \cdot \mathrm{m} \tag{7}$$

$$Q_{abs} = C_{th} \cdot \Delta\mathrm{T} \tag{8}$$

where c, 502.416 J/(kg·K), m and ΔT represent the heat capacity, mass and temperature difference of the steel mould. The calculated thermal mass of the mould is 866.2 J/K and the energy absorbed by the mould through the entire curing cycle would be 95.9 kJ. Therefore, it can be expected that with an alternative mould of less heat capacity, the heating performance could be further improved with reduced energy absorption from the mould.

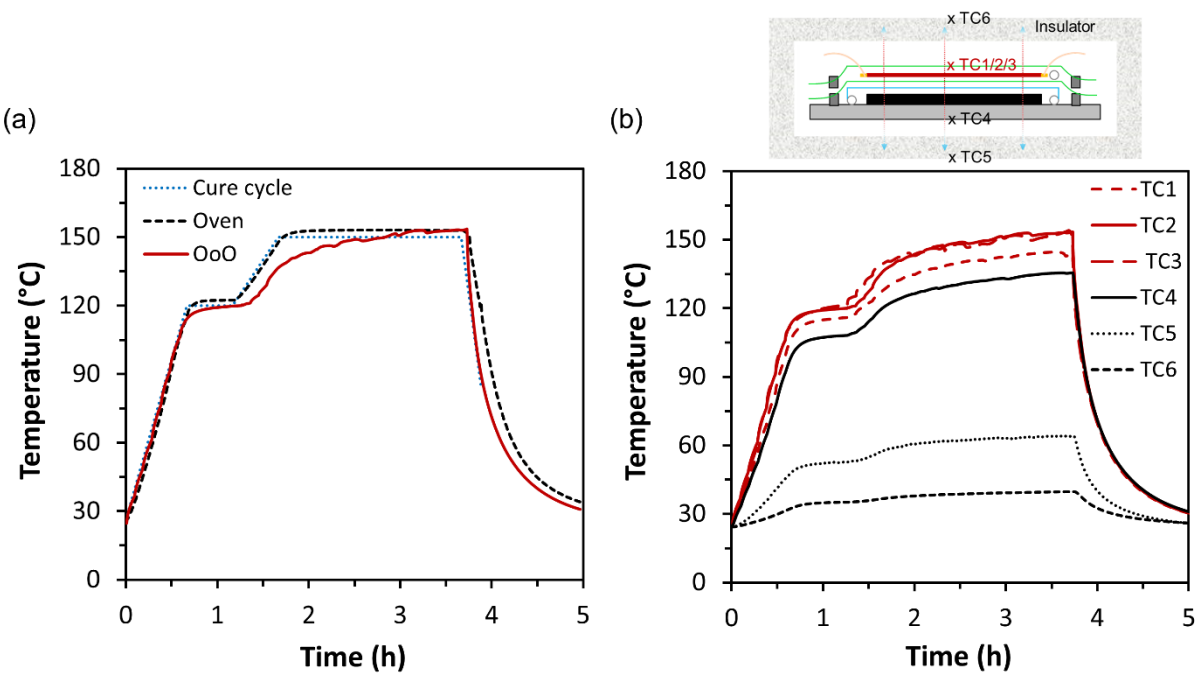

Fig. 4. (a) Comparison of heating profile between oven and OoO curing methods, both selected TC2, the central thermocouple on the surface of the whole assembly; (b) Temperature profile of the OoO curing assembly, with six thermocouples embedded at different locations: TC1/2/3 at three different positions on the surface of the heating film; TC4 was adhered to the bottom of the steel mould; TC5 and 6 were placed between the 7th and 8th layer of the insulating fabric.

3.3.2 Performance of carbon/epoxy laminates cured by both methods

Regardless of the curing methods employed, it is essential to ensure the performance of the cured laminates remains unchanged. Both the mechanical and thermomechanical performance of the cured laminates have been examined and compared for two methods.

Flexural properties of cured carbon fibre/epoxy laminates were characterized by three-point bending tests, with representative stress-strain curves, average flexural strength and modulus are summarized in Fig. 5. All samples showed comparable flexural properties, without any obvious difference in their flexural properties. Additionally, the fibre volume fractions (V_f) of oven and OoO cured carbon fibre/epoxy laminates were calculated (details in SI) with the average values at 45.0% and 46.6% respectively. The slightly higher fibre volume fraction of the OoO cured carbon fibre/epoxy laminates led to slightly higher strength (4.3%) and modulus (4.9%), which could be attributed to the second vacuum bagging procedure of attaching the heating film. DSC and DMA analysis were utilised to evaluate the thermal and thermomechanical performance of both oven and OoO cured laminates, with the results summarized in Fig. S2 and Table S2. In short, both methods gave similar T_g and storage modulus at room temperature (48 GPa and 50 GPa for oven and OoO cured laminates). These results are consistent with flexural properties. Compared with traditional oven heating, a comparable result has been obtained from the OoO method, confirming its potential as an alternative curing method for composite laminates.

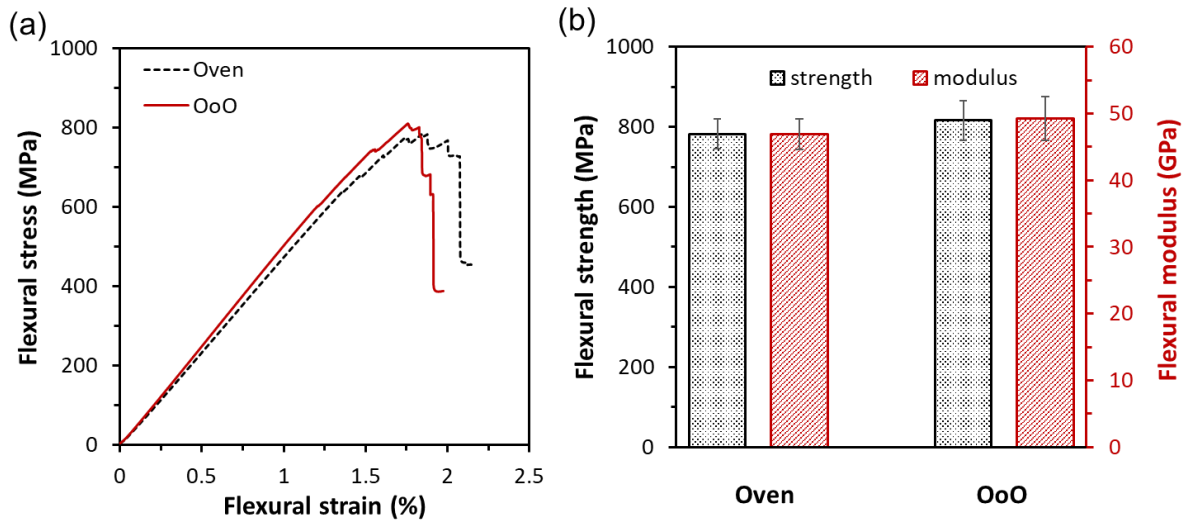

Fig. 5. (a) Representative stress-strain curves; and (b) flexural strength and modulus of carbon fibre/epoxy laminates, showing similar mechanical performance between laminates cured by oven and OoO methods.

3.3.3 Energy consumption

To compare the energy efficiency between oven and OoO method, real-time power consumption was recorded by power meter and calculated for the entire curing process. Total energy consumptions of both methods, with three repeats for each method, are summarized and compared in Fig. 6. Compared with traditional oven curing (2.3 kWh from each repeat), only 3% of energy was consumed from OoO curing method (0.073 kWh), showing a significantly reduced energy consumption. This is believed due to the conduction heating from the heating film attached to the surface of carbon fibre/epoxy laminates, alongside thermal insulation, ensuring a highly efficient heat transfer from Joule heating layer to the composite laminate. In contrast, traditional oven needs to heat up the air in the oven first before the heat can be transferred to the laminates, with most energy consumed on heating up the oven container. The

power density of 0.24 W/cm^2 and 0.30 W/cm^2 were calculated for the heating film (84 cm^2) at two steady-state curing stages, 120°C and 150 °C, respectively, which are relatively low compared to literatures with similar temperatures [13,15,18,38,39]. It is also worth noting that the amount of energy absorbed by the stainless steel mould throughout the curing was calculated to be 95.9 kJ, which was about 36% of the overall energy consumption. This could be optimized by using a mould with lower thermal mass, hence to further increase the energy efficiency of the manufacturing process.

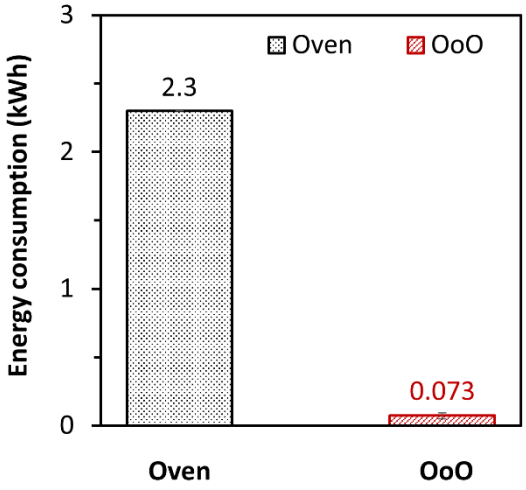

Fig. 6. Comparison of energy consumption between oven and OoO method, indicating a significant energy reduction (97%) from OoO curing method.

4. Conclusions

This work developed a tailored OoO curing method for sustainable manufacturing of high performance carbon fibre/epoxy laminates, via a two-stage self-regulating heating based on the double PTC effect. Systematic studies on both single and double PTC effects were performed, with morphological analysis to understand their pyroresistive behaviours. Single PTC intensity

of 2.1 and 1.1 was achieved at 120 °C and 160 °C, from GNP/HDPE and GNP/PVDF nanocomposites, respectively, while a double PTC with intensity of 0.6 for both stages was successfully achieved from developed GNP/HDPE/PVDF ternary nanocomposites after turning the morphology and nanofiller network. Subsequently, a two-stage self-regulating heating has been developed based on ternary nanocomposites, with heating temperature of around 120 °C and 150 °C which corresponds to the curing temperatures of epoxy resins. The relationship between applied voltage and temperature was also characterised and compared for developed system.

The tailored ternary nanocomposites with double PTC effect were utilised as an energy efficient and safe manufacturing method for high performance carbon fibre/epoxy laminates out-of-oven (OoO) curing, fulfilling both curing and post-curing temperatures with self-regulating heating. Compared with traditional oven heating, a similar heating profile was achieved from OoO method, leading to comparable mechanical and thermomechanical properties of the laminates cured by both methods. In addition, only 3% of energy consumption was used from OoO method, indicating a significantly enhanced energy efficiency from developed curing method based on nanocomposite. A relatively low power density in the range of 0.2 to 0.3 W/cm^2 was achieved. With many favoured features ranging from significantly reduced energy consumption, enhanced safety via self-regulating heating, and out-of-oven nature without size limitations, this work provides a promising route for sustainable manufacturing of high performance composites.

Supporting Information

TGA analysis of GNP nanocomposites; DSC and DMA results, thermal and thermomechanical performance of both oven and OoO cured CFRPs; Fibre volume fraction calculation of cured CFRPs.

Acknowledgements

This work was supported by the Engineering and Physical Sciences Research Council (EPSRC) [ESTEEM, EP/V037234/1]. We would like to acknowledge the great assistance from Ms Jun Ma at QMUL on the LabVIEW programming.

References

1. Galos, J. Microwave Processing of Carbon Fibre Polymer Composites: A Review. *Polym Polym Compos* **2021**, *29* (3), 151–162. https://doi.org/10.1177/0967391120903894.

2. Mgbemena, C. O.; Li, D.; Lin, M. F.; Liddel, P. D.; Katnam, K. B.; Kumar, V. T.; Nezhad, H. Y. Accelerated Microwave Curing of Fibre-Reinforced Thermoset Polymer Composites for Structural Applications: A Review of Scientific Challenges. *Compos Part A Appl Sci Manuf* **2018**, *115*, 88–103. https://doi.org/10.1016/j.compositesa.2018.09.012.

3. Zhou, J.; Li, Y.; Li, N.; Liu, S.; Cheng, L.; Sui, S.; Gao, J. A Multi-Pattern Compensation Method to Ensure Even Temperature in Composite Materials during Microwave Curing Process. *Compos Part A Appl Sci Manuf* **2018**, *107*, 10–20. https://doi.org/10.1016/j.compositesa.2017.12.017.

4. Collinson, M. G.; Bower, M. P.; Swait, T. J.; Atkins, C. P.; Hayes, S. A.; Nuhiji, B. Novel Composite Curing Methods for Sustainable Manufacture: A Review. *Compos Part C Open* **2022**, *9*, 100293. https://doi.org/10.1016/j.jcomc.2022.100293.

5. Bayerl, T.; Duhovic, M.; Mitschang, P.; Bhattacharyya, D. The Heating of Polymer Composites by Electromagnetic Induction - A Review. *Compos Part A Appl Sci Manuf* **2014**, *57*, 27–40. https://doi.org/10.1016/j.compositesa.2013.10.024.

6. Rudolf, R.; Mitschang, P.; Neitzel, M. Induction Heating of Continuous Carbon-Fibre-Reinforced Thermoplastics. *Compos Part A Appl Sci Manuf* **2000**, *31*, 1191–1202.

7. Robertson, I. D.; Yourdkhani, M.; Centellas, P. J.; Aw, J. E.; Ivanoff, D. G.; Goli, E.; Lloyd, E. M.; Dean, L. M.; Sottos, N. R.; Geubelle, P. H.; Moore, J. S.; White, S. R. Rapid Energy-Efficient Manufacturing of Polymers and Composites via Frontal Polymerization. *Nature* **2018**, *557* (7704), 223–227. https://doi.org/10.1038/s41586-018-0054-x.

8. Naseri, I.; Yourdkhani, M. Rapid and Energy-Efficient Frontal Curing of Multifunctional Composites Using Integrated Nanostructured Heaters. *ACS Appl Mater Interfaces* **2022**, *14*(44), 50215-50224. https://doi.org/10.1021/acsami.2c15415.

9. Centellas, P. J.; Yourdkhani, M.; Vyas, S.; Koohbor, B.; Geubelle, P. H.; Sottos, N. R. Rapid Multiple-Front Polymerization of Fiber-Reinforced Polymer Composites. *Compos Part A Appl Sci Manuf* **2022**, *158*, 106931. https://doi.org/10.1016/j.compositesa.2022.106931.

10. Ding, Y.; Chiu, W. K.; Liu, X. L.; Whittingham, B. Modelling of Thermal Response of Oil-Heated Tools Due to Different Flow Rates for the Manufacture of Composite Structures. Compos Struct **2001**, 54, 477–488. https://doi.org/10.1016/S0263-8223(01)00120-9.

11. Grove, S.; Summerscales, J. Heated Tooling for Aerospace Composites Manufacture. SAMPE Journal **2005**, 41 (7), 36-45. https://dx.doi.org/10.24382/4807.

12. Abdalrahman, R. Design and Analysis of Integrally-Heated Tooling for Polymer Composites, PhD Thesis, **2015**. https://doi.org/10.24382/4919.

13. Xu, X.; Zhang, Y.; Jiang, J.; Wang, H.; Zhao, X.; Li, Q.; Lu, W. In-Situ Curing of Glass Fiber Reinforced Polymer Composites via Resistive Heating of Carbon Nanotube Films. *Compos Sci Technol* **2017**, *149*, 20–27. https://doi.org/10.1016/j.compscitech.2017.06.001.

14. Lee, J.; Ni, X.; Daso, F.; Xiao, X.; King, D.; Gómez, J. S.; Varela, T. B.; Kessler, S. S.; Wardle, B. L. Advanced Carbon Fiber Composite Out-of-Autoclave Laminate Manufacture via Nanostructured out-of-Oven Conductive Curing. *Compos Sci Technol* **2018**, *166*, 150–159. https://doi.org/10.1016/j.compscitech.2018.02.031.

15. Lee, J.; Stein, I. Y.; Kessler, S. S.; Wardle, B. L. Aligned Carbon Nanotube Film Enables Thermally Induced State Transformations in Layered Polymeric Materials. *ACS Appl Mater Interfaces* **2015**, *7* (16), 8900–8905. https://doi.org/10.1021/acsami.5b01544.

16. Li, X.; Daso, F.; Lee, J.; Spangler, J.; Canart, J.-P.; Kinsella, M.; Wardle, B. L. Consolidation of Aerospace-Grade High-Temperature Thermoplastic Carbon Fiber Composites via Nano-Engineered Electrothermal Heating. *Compos B Eng* **2023**, *262*, 110814. https://doi.org/10.1016/j.compositesb.2023.110814.

17. Mas, B.; Fernández-Blázquez, J. P.; Duval, J.; Bunyan, H.; Vilatela, J. J. Thermoset Curing through Joule Heating of Nanocarbons for Composite Manufacture, Repair and Soldering. *Carbon* **2013**, *63*, 523–529. https://doi.org/10.1016/j.carbon.2013.07.029.

18. Yang, P.; Ghosh, S.; Xia, T.; Wang, J.; Bissett, M. A.; Kinloch, I. A.; Barg, S. Joule Heating and Mechanical Properties of Epoxy/Graphene Based Aerogel Composite. *Compos Sci Technol* **2022**, *218*, 109199. https://doi.org/10.1016/j.compscitech.2021.109199.

19. Xia, T.; Zeng, D.; Li, Z.; Young, R. J.; Vallés, C.; Kinloch, I. A. Electrically Conductive GNP/Epoxy Composites for out-of-Autoclave Thermoset Curing through Joule Heating. *Compos Sci Technol* **2018**, *164*, 304–312. https://doi.org/10.1016/j.compscitech.2018.05.053.

20. Vertuccio, L.; De Santis, F.; Pantani, R.; Lafdi, K.; Guadagno, L. Effective De-Icing Skin Using Graphene-Based Flexible Heater. *Compos B Eng* **2019**, *162*, 600–610. https://doi.org/10.1016/j.compositesb.2019.01.045.

21. Md, K.; Billah, M.; Hassen, A. A.; Nasirov, A.; Haye, G.; Heineman, J.; Kunc, V.; Kim, S. Thermal Analysis of Large Area Additive Manufacturing Resistance Heating Composites for out of Oven/Autoclave Applications. In *Proceedings of the ASME* **2020**, *International Mechanical Engineering Congress and Exposition, IMECE2020*.

22. Wang, Y.; Yao, X.; Thorn, T. D. S.; Huo, S.; Porwal, H.; Newton, M.; Liu, Y.; Papageorgiou, D.; Bilotti, E.; Zhang, H. Energy Efficient Out-of-Oven Manufacturing of Natural Fibre Composites with Integrated Sensing Capabilities and Improved Water Barrier Properties. *Compos Sci Technol* **2023**, *239*, 110062. https://doi.org/10.1016/j.compscitech.2023.110062.

23. Liu, Y.; Asare, E.; Porwal, H.; Barbieri, E.; Goutianos, S.; Evans, J.; Newton, M.; Busfield, J. J. C.; Peijs, T.; Zhang, H.; Bilotti, E. The Effect of Conductive Network on Positive Temperature Coefficient Behaviour in Conductive Polymer Composites. *Compos Part A Appl Sci Manuf* **2020**, *139*, 106074. https://doi.org/10.1016/j.compositesa.2020.106074.

24. Liu, Y.; Zhang, H.; Porwal, H.; Tu, W.; Wan, K.; Evans, J.; Newton, M.; Busfield, J. J. C.; Peijs, T.; Bilotti, E. Tailored Pyroresistive Performance and Flexibility by Introducing a Secondary Thermoplastic Elastomeric Phase into Graphene Nanoplatelet (GNP) Filled Polymer Composites for Self-Regulating Heating Devices. *J Mater Chem C Mater* **2018**, *6* (11), 2760–2768. https://doi.org/10.1039/c7tc05621d.

25. Liu, Y.; Zhang, H.; Porwal, H.; Busfield, J. J. C.; Peijs, T.; Bilotti, E. Pyroresistivity in Conductive Polymer Composites: A Perspective on Recent Advances and New Applications. *Polym Int* **2019**, *68* (3), 299–305. https://doi.org/10.1002/pi.5735.

26. Liu, Y.; Zhang, H.; Porwal, H.; Tu, W.; Evans, J.; Newton, M.; Busfield, J. J. C.; Peijs, T.; Bilotti, E. Universal Control on Pyroresistive Behavior of Flexible Self-Regulating Heating Devices. *Adv Funct Mater* **2017**, *27* (39), 1702253. https://doi.org/10.1002/adfm.201702253.

27. Liu, Y.; van Vliet, T.; Tao, Y.; Busfield, J. J. C.; Peijs, T.; Bilotti, E.; Zhang, H. Sustainable and Self-Regulating out-of-Oven Manufacturing of FRPs with Integrated Multifunctional Capabilities. *Compos Sci Technol* **2020**, *190*, 108032. https://doi.org/10.1016/j.compscitech.2020.108032.

28. Zhang, X.; Pan, Y. A Novel Polymer Composite with Double Positive-Temperature-Coefficient Transitions: Effect of Filler-Matrix Interface on the Resistivity-Temperature Behavior. *Polym Int* **2008**, *57* (5), 770–777. https://doi.org/10.1002/pi.2408.

29. Zhang, X. W.; Pan, Y.; Zheng, Q.; Yi, X. S. New Polymer Composite Thermistor Having Double PTC Transitions. *J Appl Polym Sci* **2000**, *78* (2), 424–429. https://doi.org/10.1002/1097-4628(20001010)78:2<424::AID-APP220>3.0.CO;2-6.

30. Hou, Y. L.; Zhang, P.; Xie, M. M. Thermally Induced Double-Positive Temperature Coefficients of Electrical Resistivity in Combined Conductive Filler–Doped Polymer Composites. *J Appl Polym Sci* **2017**, *134* (23), 44876. https://doi.org/10.1002/app.44876.

31. Zhang, P.; Hou, Y.; Wang, B. VO2-Enhanced Double Positive Temperature Coefficient Effects of High Density Polyethylene/Graphite Composites. *Mater Res Express* **2019**, *6* (3) 035702. https://doi.org/10.1088/2053-1591/aaf589.

32. Zhang, X.; Zheng, S.; Zou, H.; Zheng, X.; Liu, Z.; Yang, W.; Yang, M. Two-Step Positive Temperature Coefficient Effect with Favorable Reproducibility Achieved by Specific "Island-Bridge" Electrical Conductive Networks in HDPE/PVDF/CNF Composite. *Compos Part A Appl Sci Manuf* **2017**, *94*, 21–31. https://doi.org/10.1016/j.compositesa.2016.12.001.

33. Wei, Y.; Li, Z.; Liu, X.; Dai, K.; Zheng, G.; Liu, C.; Chen, J.; Shen, C. Temperature-Resistivity Characteristics of a Segregated Conductive CB/PP/UHMWPE Composite. *Colloid Polym Sci* **2014**, *292* (11), 2891–2898. https://doi.org/10.1007/s00396-014-3334-5.

34. Feng, J.; Chan, Chi.-M. Double Positive Temperature Coefficient Effects of Carbon Black-Filled Polymer Blends Containing Two Semicrystalline Polymers. *Polymer* **2000**, *41*(12), 4559–4565. https://doi.org/10.1016/S0032-3861(99)00690-4.

35. Yao, X.; Hawkins, S. C.; Falzon, B. G. An Advanced Anti-Icing / De-Icing System Utilizing Highly Aligned Carbon Nanotube Webs. *Carbon* **2018**, *136*, 130-138. https://doi.org/10.1016/j.carbon.2018.04.039.

36. Gupta, T. K.; Choosri, M.; Varadarajan, K. M.; Kumar, S. Self-Sensing and Mechanical Performance of CNT/GNP/UHMWPE Biocompatible Nanocomposites. *J Mater Sci* **2018**, *53* (11), 7939–7952. https://doi.org/10.1007/s10853-018-2072-3.

37. Kashi, S.; Gupta, R. K.; Kao, N.; Hadigheh, S. A.; Bhattacharya, S. N. Influence of Graphene Nanoplatelet Incorporation and Dispersion State on Thermal, Mechanical and Electrical Properties of Biodegradable Matrices. *J Mater Sci Technol* **2018**, *34* (6), 1026–1034. https://doi.org/10.1016/j.jmst.2017.10.013.

38. Raji, A. R. O.; Varadhachary, T.; Nan, K.; Wang, T.; Lin, J.; Ji, Y.; Genorio, B.; Zhu, Y.; Kittrell, C.; Tour, J. M. Composites of Graphene Nanoribbon Stacks and Epoxy for Joule Heating and Deicing of Surfaces. *ACS Appl Mater Interfaces* **2016**, *8* (5), 3551–3556. https://doi.org/10.1021/acsami.5b11131.

39. Tembei, S. A. N.; Hessein, A.; El-Bab, A. M. R. F.; El-Moneim, A. A. A Low Voltage, Flexible, Graphene-Based Electrothermal Heater for Wearable Electronics and Localized Heating Applications. *Mater Today Proc* **2020**, *33*, 1840–1844. https://doi.org/10.1016/j.matpr.2020.05.182.

Table of Contents